

# Steepest Growth in the Primordial Power Spectrum from Excited States at a Sudden Transition

Mattia Cielo,<sup>a,b,c</sup> Gianpiero Mangano,<sup>a,b</sup> Ofelia Pisanti,<sup>a,b</sup> David Wands<sup>d</sup>

<sup>a</sup>INFN - Sezione di Napoli, Complesso Univ. Monte S. Angelo, I-80126 Napoli, Italy

<sup>b</sup>Dipartimento di Fisica “Ettore Pancini”, Università degli studi di Napoli “Federico II”, Complesso Univ. Monte S. Angelo, I-80126 Napoli, Italy

<sup>c</sup>Instituto de Física Teórica UAM/CSIC, calle Nicolás Cabrera 13-15, Cantoblanco, 28049, Madrid, Spain

<sup>d</sup>Institute of Cosmology and Gravitation, Dennis Sciama Building, University of Portsmouth, PO1 3FX, United Kingdom

E-mail: [mattia.cielo@na.infn.it](mailto:mattia.cielo@na.infn.it)

**Abstract.** Sudden phase transitions during inflation can give rise to strongly enhanced primordial density perturbations on scales much smaller than those directly probed by cosmic microwave background anisotropies. In this paper, we study the effect of the incoming quantum state on the steepest growth found in the primordial power spectrum using a simple model of an instantaneous transition during single-field inflation. We consider the case of a general de Sitter-invariant initial state for the inflaton field (the  $\alpha$ -vacuum), and also an incoming state perturbed by a preceding transition. For the  $\alpha$ -vacua we find that  $k^6$  growth is possible for  $\alpha > 0$ , while  $k^4$  growth is seen for  $\alpha \leq 0$ , including the standard case of an initial Bunch-Davies vacuum state. The features of an enhanced primordial power spectrum on small scales are thus sensitive to the initial quantum state during inflation. We calculate the scalar-induced gravitational wave power spectrum for each case.

---

## Contents

<b>1</b>	<b>Introduction</b>	<b>1</b>
<b>2</b>	<b>Single sudden transition during inflation</b>	<b>2</b>
2.1	Starobinsky piecewise-linear potential	4
2.1.1	Bunch-Davies initial state	6
2.1.2	$\alpha$ -vacuum initial state	8
2.1.3	Scalar-induced gravitational waves	10
<b>3</b>	<b>Generalization for multiple transitions</b>	<b>11</b>
3.1	$n$ transitions	11
3.2	Two transitions	13
<b>4</b>	<b>Conclusions</b>	<b>14</b>

---

## 1 Introduction

What is the steepest growth of the primordial scalar power spectrum after an inflationary stage? This question has received considerable attention [1–7] since the abundance and mass spectrum of primordial black holes (PBHs) and the associated stochastic gravitational wave (GW) background [8] are known to be sensitive to the shape of the primordial power spectrum as well as the height of its peak [9–15]. A consistent interpretation of observational bounds requires a treatment that goes beyond the simplistic assumption of an almost monochromatic scalar power spectrum [3, 7, 11, 16]. Previous work argued that rapid growth in the power spectrum is expected to be at most  $\sim k^4$  [1, 6], while subsequently it was argued that  $\sim k^5(\log k)^2$  was the steepest possible growth [2]. Such strong scale-dependence necessarily requires features in the inflaton potential and/or sound speed, leading to a sudden phase transition and the breakdown of slow roll, mixing adiabatic and isocurvature modes of the scalar field perturbations [17]. Tasinato has shown [4] that multiple transitions during inflation can lead to much stronger enhancements in the power spectrum, indicating that the slope of the spectrum has a memory of the history of non-slow-roll phases during inflation. Sudden (non-adiabatic) phase transitions lead to particle production and a non-trivial incoming quantum state which can be amplified at subsequent transitions. Motivated by these considerations and recent developments in the study of non-Bunch-Davies initial states of quantum perturbations [18–30], we will extend the analysis proposed in Ref. [1] by incorporating the additional degeneracy inherent in quantum field theory on curved spacetime. It is well understood in fact that after the quantum-to-classical transition for the cosmological perturbations, the choice of the initial vacuum state is quite crucial [31]. In particular, we study the so-called  $\alpha$ -vacua corresponding to de Sitter invariant initial states [32]. This extension allows us to explore a broader range of scenarios and enrich our understanding of the quantum field dynamics. We will study an idealised model of an instantaneous transition driven by a piecewise-linear potential, originally proposed by Starobinsky [33], which provides a simple realisation of an inflationary model with a sudden transition from slow-roll to ultra-slow-roll, leading to a rapid growth in the primordial power spectrum. This model, despite its simplicity, can exhibit a

rich phenomenology in the resulting primordial power spectrum for the scalar curvature perturbations and yield non-trivial results for both the production of the primordial black holes and the scalar-induced gravitational waves at second order. The paper is organized as follows. In section 2 we introduce all the essential quantities needed to study the primordial scalar spectrum at the end of inflation, and give the general expressions for matching Bogoliubov coefficient across a sudden transition. We then introduce the Starobinsky piecewise-linear potential and emphasize the role of the choice of the incoming quantum state. We show analytically how the growth of the power spectrum can be estimated from the relation between the Bogoliubov coefficients before and after a sudden transition. We study the shape of the scalar power spectra resulting from different choices for the initial  $\alpha$ -vacua and the impact that this has on the stochastic GW background produced at second order. We calculate the effective GW energy density,  $\Omega_{GW}$ , using the public code SIGWfast [34]. In section 3 we generalize Starobinsky’s model of a single transition to a piecewise-linear potential including an arbitrary number of transitions and derive a general recurrence formula for obtaining the Bogoliubov coefficients after each step as functions of the previous ones. We then apply this analysis to the specific case of  $n = 2$  transitions. We conclude in section 4.

## 2 Single sudden transition during inflation

We work within the single-field paradigm of cosmic inflation. Specifically, we consider a minimally-coupled inflaton field governed by the Klein-Gordon equation in a Friedmann-Lemaitre-Robertson-Walker (FLRW) cosmology

$$\ddot{\phi} + 3H\dot{\phi} + \frac{dV}{d\phi} = 0, \quad (2.1)$$

where the Hubble rate  $H \equiv \dot{a}/a$  is given by the Friedmann constraint

$$H^2 = \frac{8\pi}{3} \left( V + \frac{1}{2}\dot{\phi}^2 \right). \quad (2.2)$$

The inflationary dynamics can be described in terms of two dimensionless slow-roll parameters

$$\epsilon_1 \equiv -\frac{\dot{H}}{H^2}, \quad \epsilon_2 \equiv \frac{\dot{\epsilon}_1}{\epsilon_1 H} = -6 - \frac{2}{H\dot{\phi}} \frac{dV}{d\phi}, \quad (2.3)$$

where we require  $\epsilon_1 < 1$  for an accelerated expansion. We will work in the quasi-de Sitter limit, in which  $\epsilon_1 \rightarrow 0$  so  $H$  is effectively constant, but we will allow  $\epsilon_1$  to vary in time, hence  $\epsilon_2$  is not necessarily small. It is small in the usual slow-roll approximation ( $|\epsilon_2| \ll 1$ ), but becomes large during a period of ultra-slow roll inflation ( $\epsilon_2 \approx -6$ ) [35]. Each wave mode of the curvature perturbation,  $\mathcal{R}$ , with comoving wavenumber  $k$ , obeys the evolution equation

$$\mathcal{R}_k'' + 2\frac{z'}{z}\mathcal{R}_k + k^2\mathcal{R}_k = 0, \quad (2.4)$$

where  $z(\tau) \equiv a\dot{\phi}/H$  and primes denote derivatives with respect to conformal time,  $\tau = \int dt/a$ . Note that in de Sitter ( $\epsilon_1 \rightarrow 0$ ) we have  $a = -1/H\tau$  and thus  $\tau$  runs from  $-\infty$  to 0 as  $a$  evolves from 0 to  $\infty$ . Through a suitable rescaling,  $v = \mathcal{R}/z$ , we can cast (2.4) into the Sasaki-Mukhanov mode equation

$$v_k'' + \left( k^2 - \frac{z''}{z} \right) v_k = 0. \quad (2.5)$$

This second-order differential equation is solved by a linear combination of two independent solutions, which can be written as

$$v_k(\tau) = \frac{\mathcal{A}_k f_k(\tau) + \mathcal{B}_k f_k^*(\tau)}{\sqrt{2k}}, \quad (2.6)$$

where the complex functions  $f_k(\tau)$  are normalised such that the Wronskian obeys  $f_k^* f_k' - f_k'^* f_k = 2ik$ . In particular we will require that  $f_k(\tau) \rightarrow e^{-ik\eta}$  in the short-wavelength limit  $(z''/z)/k^2 \rightarrow 0$ . The commutation relations for the corresponding quantum field operator,  $\hat{v}$ , and its canonical momentum then require

$$|\mathcal{A}_k|^2 - |\mathcal{B}_k|^2 = 1. \quad (2.7)$$

Finally, we must specify the initial state of the field, which determines the behaviour of the quantum operator,  $\hat{v}$ , on the ground state of the theory,  $|0\rangle$ . The most common choice is the Bunch-Davies vacuum ( $\mathcal{A}_k = 1, \mathcal{B}_k = 0$ ) which corresponds to the minimum energy state [36], but for now, we will leave the initial state arbitrary. We will consider models where a sudden transition occurs due to a potential,  $V(\phi)$ , which is continuous but with a sudden change in the derivative at  $\phi = \phi_1$ . We are not interested in effects coming from the detailed form of the potential around  $\phi = \phi_1$ , so we will treat the transition as instantaneous. We expect this to be a good description of wavemodes  $k \ll a/\Delta t$  where  $\Delta t$  is the duration of the transition in terms of proper time, and we define a sudden transition to be one for which  $\Delta t \ll H^{-1}$ . We thus have the junction conditions at  $\phi_1$ :

$$[V]_{-}^{+} = 0 \quad \left[ \frac{dV}{d\phi} \right]_{-}^{+} = \Delta V' \quad (2.8)$$

This leaves the field and its time derivative continuous,  $[\phi]_{-}^{+} = [\dot{\phi}]_{-}^{+} = 0$ , but the second time derivative is discontinuous,  $[\ddot{\phi}]_{-}^{+} = -\Delta V'/3H$ . Hence  $z(\tau)$  is continuous, but  $z'(\tau)$  is discontinuous:

$$[z]_{-}^{+} = 0, \quad \left[ \frac{z'}{z} \right]_{-}^{+} = -\frac{a_1 \Delta V'}{\dot{\phi}_1} \equiv \Delta_1 \quad (2.9)$$

Note that the scalar field density and pressure are continuous across the transition, but the time-derivative of the pressure is discontinuous, hence we will refer to this as a second-order phase transition (the second time-derivative of the energy density is discontinuous). From integrating the mode equation (2.9) across the transition (or from requiring the continuity of the comoving curvature perturbation,  $\mathcal{R}$ , and its derivative) we find:

$$[v_k]_{-}^{+} = 0, \quad [v_k']_{-}^{+} = -\Delta_1 v_k \quad (2.10)$$

Without loss of generality, we will require that the particular solution of the Sasaki-Mukhanov mode equation (2.5),  $f_k$ , and its derivative,  $f_k'$ , are continuous across the transition. In terms of the general solution (2.6) we thus have

$$[\mathcal{A}_k f_k + \mathcal{B}_k f_k^*]_{-}^{+} = 0, \quad (2.11)$$

$$\left[ \mathcal{A}_k f_k' + \mathcal{B}_k f_k'^* \right]_{-}^{+} = -\Delta_1 (\mathcal{A}_k f_{k1} + \mathcal{B}_k f_{k1}^*). \quad (2.12)$$

where  $f_{k1} = f_k(\tau_1)$ . Following [33] we will assume that  $\dot{\phi} < 0$  and the scalar field evolves from  $\phi > \phi_1$  to  $\phi < \phi_1$ . Before the transition, for  $\phi > \phi_1$ , we write

$$\mathcal{A}_{k+} = \mathcal{A}_k, \quad \mathcal{B}_{k+} = \mathcal{B}_k, \quad (2.13)$$

while after the transition, for  $\phi < \phi_1$ , we set

$$\mathcal{A}_{k-} = \tilde{\mathcal{A}}_k, \quad \mathcal{B}_{k-} = \tilde{\mathcal{B}}_k. \quad (2.14)$$

From Eqs. (2.11) and (2.12) we can establish a general relationship between the Bogoliubov coefficients before and after the transition<sup>1</sup>

$$\begin{bmatrix} \tilde{\mathcal{A}}_k \\ \tilde{\mathcal{B}}_k \end{bmatrix} = \begin{bmatrix} 1 - i\Delta_1 f_{k1}^* f_{k1} (2k)^{-1} & -i\Delta_1 f_{k1}^* f_{k1}^* (2k)^{-1} \\ +i\Delta_1 f_{k1} f_{k1} (2k)^{-1} & 1 + i\Delta_1 f_{k1}^* f_{k1} (2k)^{-1} \end{bmatrix} \begin{bmatrix} \mathcal{A}_k \\ \mathcal{B}_k \end{bmatrix}. \quad (2.15)$$

## 2.1 Starobinsky piecewise-linear potential

The Starobinsky piecewise-linear potential serves as a convenient illustrative example of a sudden (non-adiabatic) transition [33]. This model is characterized by the potential:

$$V(\phi) = \begin{cases} V_0 + A_1(\phi - \phi_1), & \phi > \phi_1 \\ V_0 + A_2(\phi - \phi_1), & \phi < \phi_1 \end{cases} \quad (2.16)$$

In our scenario,  $\dot{\phi} < 0$  and  $A_1 = A_+ > 0$  represents the slope of the potential before the transition and  $A_2 = A_-$  represents the slope after the transition at  $\phi = \phi_1$ . We assume that during the initial regime,  $\phi > \phi_1$ , our field follows a slow-roll evolution. In this regime, we can neglect the acceleration term in the Klein-Gordon equation (2.1), leading to the friction being equal and opposite to the potential slope

$$\dot{\phi} \simeq -\frac{A_1}{3H} \quad \text{for } \phi > \phi_1. \quad (2.17)$$

Since we will assume that we are close to de Sitter throughout, we require  $A_1 \ll M_{Pl}H^2$  and thus during slow roll both  $\epsilon_1 \ll 1$  and  $|\epsilon_2| \ll 1$ . When the field reaches  $\phi = \phi_1$  there is a sudden change in the potential gradient,  $\Delta V' = A_1 - A_2$ . After the transition ( $t > t_1$ ) the Klein-Gordon equation (2.1) can be integrated to give the simple solution:

$$\dot{\phi} = -\left(\frac{A_1 - A_2}{3H}\right) e^{-3H(t-t_1)} - \frac{A_2}{3H} \quad \text{for } \phi < \phi_1. \quad (2.18)$$

For  $0 < A_2 \ll A_1$  the potential gradient becomes much smaller than the friction term immediately after the transition, and the slow-roll approximation is no longer applicable. In this phase the field's deceleration is driven by the friction term,  $\ddot{\phi} \approx -3H\dot{\phi}$ , violating slow roll and, from Eq. (2.3), leading to  $\epsilon_2 \approx -6$ , while  $\epsilon_1$  remains small. This is commonly referred to as Ultra-Slow Roll inflation (USR) [35]. However, this USR phase is transient, as the time-derivative of the scalar field decays rapidly,  $\dot{\phi} \propto e^{-3Ht}$ , and hence the field's acceleration also decays rapidly, and at late times the system approaches a new slow-roll attractor with  $3H\dot{\phi} \simeq -A_2$  and  $|\epsilon_2| \ll 1$ . To compute the primordial power spectrum, we solve the Mukhanov-Sasaki mode equation (2.5) before and after the transition. For the

<sup>1</sup>It is straightforward to check that the normalisation condition (2.7) still holds after the transition, as it should for a quantum field, and we have  $|\tilde{\mathcal{A}}_k|^2 - |\tilde{\mathcal{B}}_k|^2 = 1$ .

piece-wise linear potential (2.16), corresponding to a massless inflaton field in the de Sitter limit ( $\epsilon_1 \rightarrow 0$ ), the time-dependent mass in the mode equation (2.5),  $z''/z = 2/\tau^2$ , remains invariant [37, 38] before and after the transition at  $\phi = \phi_1$ . Thus the general solution to the mode equation is given by the expression in Eq. (2.6) where in both regimes

$$f_k(\tau) = \left(1 - \frac{i}{k\tau}\right) e^{-ik\tau}. \quad (2.19)$$

We see that on small scales and at early times ( $k\tau \rightarrow -\infty$ )  $f_k \rightarrow e^{-ik\tau}$ , while on large scales and late times ( $k\tau \rightarrow 0$ )  $f_k = -f_k^* \rightarrow -i/k\tau$ . Thus the dimensionless power spectrum for the primordial curvature perturbation is

$$\mathcal{P}_{\mathcal{R}}(k) = \frac{4\pi k^3 |v_k^2|}{(2\pi)^3 z^2}, \quad (2.20)$$

Before the transition, in slow roll, the initial conditions for the modes are set by the choice of the vacuum state, e.g., the Bunch-Davies vacuum, where  $\mathcal{A}_k = 1$  and  $\mathcal{B}_k = 0$ , and we recover the scale-invariant power spectrum  $\mathcal{P}_{\mathcal{R}} = (H^2/2\pi\dot{\phi})^2$ . However at late times, after the transition, the power spectrum is given by [39]

$$\mathcal{P}_{\mathcal{R}}(k) \rightarrow \left(\frac{H^2}{2\pi\dot{\phi}}\right)^2 |\tilde{\mathcal{A}}_k - \tilde{\mathcal{B}}_k|^2 \quad \text{as } k\tau \rightarrow 0. \quad (2.21)$$

The matrix (2.15) matching the Bogoliubov coefficients across the sudden transition, using the mode function (2.19) for a free field in de Sitter, becomes

$$\begin{bmatrix} \tilde{\mathcal{A}}_k \\ \tilde{\mathcal{B}}_k \end{bmatrix} = \begin{bmatrix} 1 - (i\Delta_1/2k_1)(1 + \kappa^2)/\kappa^3 & (i\Delta_1/2k_1)(1 + i\kappa)^2 e^{-2i\kappa}/\kappa^3 \\ -(i\Delta_1/2k_1)(1 - i\kappa)^2 e^{2i\kappa}/\kappa^3 & 1 + (i\Delta_1/2k_1)(1 + \kappa^2)/\kappa^3 \end{bmatrix} \begin{bmatrix} \mathcal{A}_k \\ \mathcal{B}_k \end{bmatrix}, \quad (2.22)$$

where  $k_1$  represents the wavenumber crossing outside the Hubble scale at the time of the transition,  $k_1 = a_1 H$ , and here and in the following equations we have introduced the normalized wavenumber  $\kappa \equiv k/k_1$ . The sudden transition in the acceleration of the field results in a discontinuity in the time-derivative of  $z(\tau)$  given by Eq. (2.9). For the piecewise linear potential (2.16) we have

$$\Delta_1 = \frac{3k_1(A_1 - A_2)}{A_1}. \quad (2.23)$$

After the transition the Bogoliubov coefficients are thus set by Eqs. (2.22), where using (2.23) we obtain

$$\begin{aligned} \tilde{\mathcal{A}}_k &= \mathcal{A}_k - \frac{3i}{2\kappa^3} \left(\frac{A_1 - A_2}{A_1}\right) \left\{ (1 + \kappa^2)\mathcal{A}_k - (1 + i\kappa)^2 e^{-2i\kappa}\mathcal{B}_k \right\}, \\ \tilde{\mathcal{B}}_k &= \mathcal{B}_k + \frac{3i}{2\kappa^3} \left(\frac{A_1 - A_2}{A_1}\right) \left\{ (1 + \kappa^2)\mathcal{B}_k - (1 - i\kappa)^2 e^{2i\kappa}\mathcal{A}_k \right\}. \end{aligned} \quad (2.24)$$

The final power spectrum (2.21) for an arbitrary initial state is determined by the combination

$$\tilde{\mathcal{A}}_k - \tilde{\mathcal{B}}_k = (\mathcal{A}_k - \mathcal{B}_k) \left\{ 1 + 3 \left(\frac{A_1 - A_2}{A_1}\right) \kappa j_1(\kappa) y_1(\kappa) \right\} - i(\mathcal{A}_k + \mathcal{B}_k) \left\{ 3 \left(\frac{A_1 - A_2}{A_1}\right) \kappa j_1^2(\kappa) \right\}, \quad (2.25)$$

where

$$j_1(\kappa) = \frac{\sin \kappa}{\kappa^2} - \frac{\cos \kappa}{\kappa}, \quad y_1(\kappa) = -\frac{\cos \kappa}{\kappa^2} - \frac{\sin \kappa}{\kappa}, \quad (2.26)$$

are spherical Bessel functions of the first and second kind. For super-Hubble modes at the transition ( $\kappa < 1$ ) we can Taylor expand (2.26), which substituted into Eq. (2.25) gives

$$\begin{aligned} \tilde{\mathcal{A}}_k - \tilde{\mathcal{B}}_k &= \left\{ \frac{A_2}{A_1} - \frac{2}{5} \left( \frac{A_1 - A_2}{A_1} \right) \kappa^2 (1 + \mathcal{O}(\kappa^2)) \right\} (\mathcal{A}_k - \mathcal{B}_k) \\ &\quad - \frac{i}{3} \left( \frac{A_1 - A_2}{A_1} \right) \kappa^3 (1 + \mathcal{O}(\kappa^2)) (\mathcal{A}_k + \mathcal{B}_k). \end{aligned} \quad (2.27)$$

We see that  $\tilde{\mathcal{A}}_k - \tilde{\mathcal{B}}_k \rightarrow (A_2/A_1)(\mathcal{A}_k - \mathcal{B}_k)$  as  $\kappa \rightarrow 0$  and the primordial power spectrum (2.21) remains unchanged in the very large-scale limit<sup>2</sup>. However, for  $A_1 \gg A_2$  there will be a rapid rise in the primordial power spectrum on a range of scales larger than the Hubble scale at the transition,  $A_2/A_1 < \kappa^2 < 1$ , with the slope depending on the incoming state, given by  $\mathcal{A}_k$  and  $\mathcal{B}_k$ .

### 2.1.1 Bunch-Davies initial state

Having obtained the general solution to the mode functions (2.6) before and after the transition, and thus the primordial power spectrum (2.20), we must now specify the initial state for the quantum field at early times. The simplest choice for the initial state is the one adopted by Bunch and Davies which is equivalent to selecting the minimum energy state for the field [36]. In this case the Bogoliubov coefficients (2.6), before the transition, take the simple form:

$$\mathcal{A}_k = 1 \quad \mathcal{B}_k = 0 \quad (2.28)$$

After the transition, the quantum state is determined by the junction conditions (2.10) leading to the new Bogoliubov coefficients (2.24) [33]

$$\tilde{\mathcal{A}}_k = 1 - \frac{3i(A_1 - A_2)}{2A_1} \frac{(1 + \kappa^2)}{\kappa^3}, \quad (2.29)$$

$$\tilde{\mathcal{B}}_k = -\frac{3i(A_1 - A_2)}{2A_1} \frac{(1 - i\kappa)^2 e^{2i\kappa}}{\kappa^3}. \quad (2.30)$$

The sudden transition (2.9) results in a state that mixes negative and positive frequency modes. It is apparent that even when starting from the Bunch-Davies vacuum state, a sudden transition ( $A_2 \neq A_1$ ) induces excitations in the modes corresponding to particle production ( $\tilde{\mathcal{B}}_k \neq 0$ ) in the inflaton field on sub-horizon scales after the transition, and non-adiabatic perturbations on super-Hubble scales [17]. Substituting Eqs (2.28) into (2.25) to compute the primordial scalar power spectrum at the end of inflation (2.21) we obtain

$$\mathcal{P}_{\mathcal{R}} = \frac{9H^6}{4\pi^2 A_1^2 A_2^2} \left\{ [A_1 + 3(A_1 - A_2)\kappa j_1(\kappa)y_1(\kappa)]^2 + [3(A_1 - A_2)\kappa j_1^2(\kappa)]^2 \right\}, \quad (2.31)$$

where

$$\kappa j_1(\kappa)y_1(\kappa) = \frac{(\kappa^2 - 1)\sin(2\kappa) + 2\kappa\cos(2\kappa)}{2\kappa^3}, \quad \kappa j_1^2(\kappa) = \frac{(\kappa\cos\kappa - \sin\kappa)^2}{\kappa^3}, \quad (2.32)$$

---

<sup>2</sup>Recall that before the transition  $\dot{\phi} = -A_1/3H$  while  $\dot{\phi} \rightarrow -A_2/3H$  as  $\tau \rightarrow 0$  after the transition

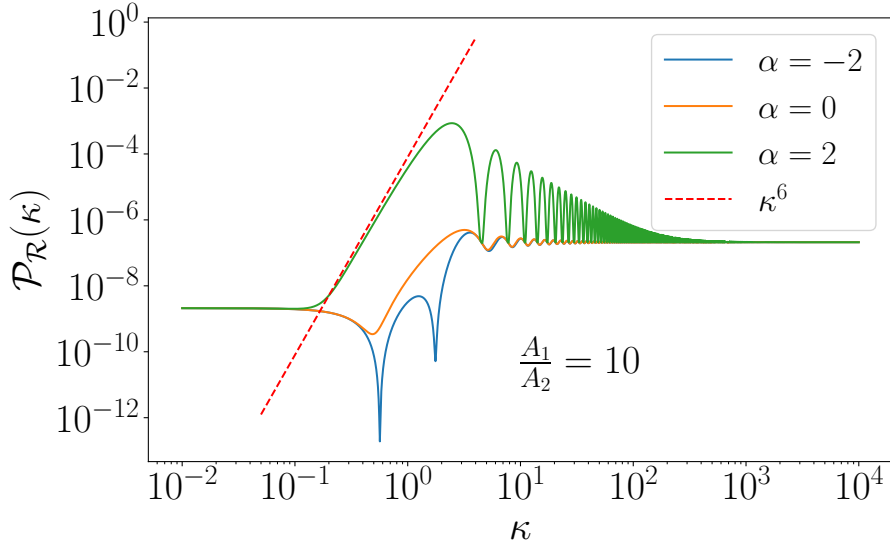


**Figure 1.** The power spectrum of the curvature perturbation  $\mathcal{P}_{\mathcal{R}}$  at the end of inflation, Eq. (2.20), as a function of the normalized wavenumber,  $\kappa = k/k_1$ , where  $k_1$  is the wavenumber which crosses the horizon at the sudden transition. The plot shows power spectra obtained for different initial  $\alpha$ -vacuum states (2.35), varying  $\alpha$  for  $\beta = 0$ . In this plot, we fix the ratio between the slopes  $A_1/A_2 = 10$  and we have fixed  $H^3 e^\alpha/A_1$  such that  $\mathcal{P}_{\mathcal{R}} \rightarrow 2 \times 10^{-9}$  for  $\kappa \rightarrow 0$ .

and we have used the late-time solution for the time-derivative of the field after the transition,  $\dot{\phi} \rightarrow -A_2/(3H)$ . The power spectrum (2.31) is shown by the middle (orange) curve in Figure 1. From the Taylor expansion on super-Hubble scales at the transition, Eq. (2.27), we see that if modes start in the Bunch-Davies vacuum state (2.28), then on very large scales,  $\kappa^2 \ll A_2/A_1 \ll 1$ , the spectrum remains scale-invariant. However for smaller scales, but still larger than the Hubble scale at the transition,  $\kappa^2 < 1$ , the real part of  $\tilde{\mathcal{A}}_k - \tilde{\mathcal{B}}_k$  in Eq. (2.27) vanishes for  $\kappa^2 \simeq (5/2)A_2/A_1$ , corresponding to a dip in the power spectrum [33, 38, 40]. This is followed by a rise in  $|\tilde{\mathcal{A}}_k - \tilde{\mathcal{B}}_k| \propto \kappa^2$ , hence a rise in  $\mathcal{P}_{\mathcal{R}} \propto \kappa^4$ , for smaller scales, but still larger than the Hubble scale [38]

$$\mathcal{P}_{\mathcal{R}} = \left( \frac{3H^3}{5\pi A_2} \right)^2 \kappa^4, \quad \text{for } \frac{A_2}{A_1} \ll \kappa^2 \ll 1. \quad (2.33)$$

The power spectrum rises to a peak at  $\kappa \sim \pi$  [33, 40] and then exhibits damped oscillations about the asymptotic value on sub-Hubble scales

$$\mathcal{P}_{\mathcal{R}} \rightarrow \frac{9H^6}{4\pi^2 A_2^2}, \quad \text{for } \kappa \rightarrow \infty. \quad (2.34)$$

Finally, we note from Eq. (2.30) that the particle number density after the transition  $k^3 |\tilde{\mathcal{B}}_k|^2 \propto \kappa$  for  $\kappa \gg 1$ . The corresponding energy density is thus formally divergent as  $\kappa \rightarrow \infty$ . This is a result of modelling the transition as instantaneous, which excites arbitrarily high energy modes. In practice the particle production will be suppressed on length scales much smaller than the duration of the transition,  $\kappa \gg a/(k_1 \Delta t)$ .



### 2.1.2 $\alpha$ -vacuum initial state

We will now extend our calculation of the primordial power spectrum to explore the additional degeneracy induced by the choice of the initial state of the quantum field (2.6). As previously remarked, the commutation relation for the field and its canonical momentum place the constraint (2.7) on the Bogoliubov coefficients. For this reason, we adopt the parametrization in terms of hyperbolic functions [32]

$$\mathcal{A}_k = \cosh(\alpha) \quad \mathcal{B}_k = e^{i\beta} \sinh(\alpha) \quad (2.35)$$

Here,  $\alpha$  is a real free parameter, characterizing the initial state within a family of degenerate  $\alpha$ -vacuum states obeying the normalisation condition (2.7). This degeneracy arises due to the absence of temporal Killing vectors in the FLRW foliation of the spacetime [41, 42]. Here we will choose  $\alpha$  and  $\beta$  to be scale-invariant (independent of the wavenumber,  $k$ ) which corresponds to a de Sitter invariant initial state [32]. The Bunch-Davies vacuum (2.28) represents the particular choice  $\alpha = 0$  for the initial state. Although we might be tempted to choose any value for the parameters  $\alpha$  and  $\beta$ , we must exercise caution to ensure that we do not disrupt the inflationary phase by introducing an excessive particle density. The particle energy density is given by [43, 44]:

$$\varepsilon_{\delta\phi} \sim \frac{1}{a^4} \int_0^{a\Lambda} dk k^3 |\mathcal{B}_k|^2 \quad (2.36)$$

where we take a physical UV cut-off,  $\Lambda$ . We need to guarantee that during the inflationary stage, the particle energy density is much less than that of the potential,  $V_0$ . Hence we require  $\sinh^2(\alpha) \ll V_0/\Lambda^4$ . In practice, we will limit our discussion to the range  $-2 \leq \alpha \leq 2$ . Using the  $\alpha$ -vacuum initial state (2.35) before the transition, we can again compute the outgoing Bogoliubov coefficients (2.24) after having applied the matching condition (2.10)

$$\begin{aligned} \tilde{\mathcal{A}}_k = & \left[ 1 - \frac{3i}{2\kappa^3} \left( \frac{A_1 - A_2}{A_1} \right) (1 + \kappa^2) \right] \cosh(\alpha) \\ & + \frac{3i}{2\kappa^3} \left( \frac{A_1 - A_2}{A_1} \right) (1 + i\kappa)^2 e^{-2i\kappa} e^{i\beta} \sinh(\alpha), \end{aligned} \quad (2.37)$$

$$\begin{aligned} \tilde{\mathcal{B}}_k = & \left[ 1 + \frac{3i}{2\kappa^3} \left( \frac{A_1 - A_2}{A_1} \right) (1 + \kappa^2) \right] e^{i\beta} \sinh(\alpha) \\ & - \frac{3i}{2\kappa^3} \left( \frac{A_1 - A_2}{A_1} \right) (1 - i\kappa)^2 e^{2i\kappa} \cosh(\alpha). \end{aligned} \quad (2.38)$$

Substituting (2.35) into (2.25) we obtain the power spectrum at the end of inflation (2.21)

$$\begin{aligned} \mathcal{P}_{\mathcal{R}} = & \frac{9H^6}{4\pi^2 A_1^2 A_2^2} \left\{ \left[ (\cosh \alpha - \cos \beta \sinh \alpha) (A_1 + 3(A_1 - A_2) \kappa j_1(\kappa) y_1(\kappa)) \right. \right. \\ & \left. \left. + 3 \sin \beta \sinh \alpha (A_1 - A_2) \kappa j_1^2(\kappa) \right]^2 \right. \\ & \left. + \left[ \sin \beta \sinh \alpha (A_1 + 3(A_1 - A_2) \kappa j_1(\kappa) y_1(\kappa)) \right. \right. \\ & \left. \left. + 3 (\cosh \alpha + \cos \beta \sinh \alpha) (A_1 - A_2) \kappa j_1^2(\kappa) \right]^2 \right\}. \end{aligned} \quad (2.39)$$

Let us first consider the case where we fix the phase  $\beta = 0$ . In this case Eq. (2.39) reduces to

$$\mathcal{P}_{\mathcal{R}} = \frac{9H^6}{4\pi^2 A_1^2 A_2^2} \left\{ e^{-2\alpha} \left[ A_1 + 3(A_1 - A_2) \kappa j_1(\kappa) y_1(\kappa) \right]^2 + e^{2\alpha} \left[ 3(A_1 - A_2) \kappa j_1^2(\kappa) \right]^2 \right\}, \quad (2.40)$$

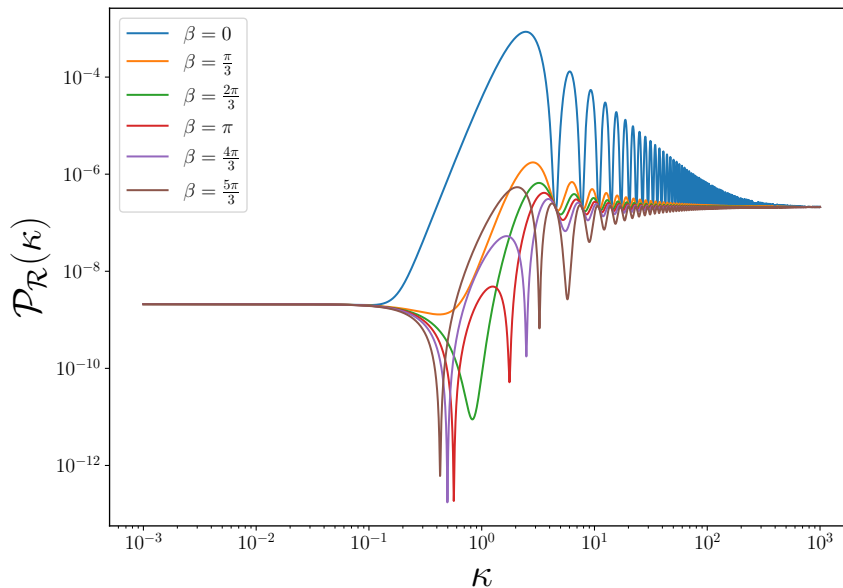


**Figure 2.** The power spectrum of the curvature perturbation  $\mathcal{P}_{\mathcal{R}}$  (2.20) as a function of the normalized wavenumber  $\kappa = k/k_1$ , where  $k_1$  is the wavenumber which crosses the horizon at the sudden transition. The plot shows different power spectra obtained by varying the  $\beta$  parameter in the initial  $\alpha$ -vacuum states (2.35), while fixing the value of  $\alpha = 2$ . In this plot, we fix the ratio between the slopes  $A_1/A_2 = 10$  and we have fixed  $H^3 e^\alpha/A_1$  such that  $\mathcal{P}_{\mathcal{R}} \rightarrow 2 \times 10^{-9}$  for  $\kappa \rightarrow 0$ .

This expression for the primordial power spectrum differs from the result for a Bunch-Davies initial state, Eq. (2.31), solely due to the presence of the two exponential functions of  $\alpha$  in Eq. (2.40). By setting  $\alpha$  to zero, we recover the standard solution from the Bunch-Davies vacuum. Figure 1 illustrates how the selection of the  $\alpha$  parameter can significantly influence the shape of the primordial spectrum (2.40) after a sudden transition. A *negative*  $\alpha$  parameter, leads to a deeper initial dip at  $\kappa_2 \simeq (5/2)A_2/A_1$ , where the real part of  $\tilde{\mathcal{A}}_k - \tilde{\mathcal{B}}_k$  in Eq. (2.27) vanishes. There is then an additional dip before the power spectrum rises to reach a peak very similar to the standard Bunch-Davies scenario, displaying similar oscillations with the same periodicity for  $\kappa \gg 1$ . Conversely, the *positive*  $\alpha$  case has no dip and gives a steeper growth reaching a significantly higher peak compared with the one obtained from the Bunch-Davies vacuum. We can understand this behaviour by writing the Taylor expansion on super-Hubble scales (2.27) for the case of a strong transition,  $A_2 \ll A_1$  to give

$$\tilde{\mathcal{A}}_k - \tilde{\mathcal{B}}_k = \left( \frac{A_2}{A_1} - \frac{2}{5}\kappa^2 + \mathcal{O}(\kappa^4) \right) e^{-\alpha} - \frac{i}{3} (\kappa^3 + \mathcal{O}(\kappa^5)) e^\alpha \quad \text{for } \kappa \ll 1. \quad (2.41)$$

We see that if we start in an  $\alpha$ -vacuum with  $e^\alpha \gg 1$  (such that  $|\mathcal{A}_k + \mathcal{B}_k| \gg |\mathcal{A}_k - \mathcal{B}_k|$ ), then the leading correction for  $(A_2/A_1)e^{-2\alpha} \ll \kappa^3 \ll 1$  becomes  $k^3$ , giving a  $k^6$  rise in the power spectrum (2.40) on super-Hubble scales at the transition, rather than the  $k^4$  rise seen for the Bunch-Davies vacuum. Because the  $\kappa^3$  term in (2.27) is out of phase with respect to the  $\kappa^0$  term, there is no longer a dip in the power spectrum between the plateau and the rise in the power spectrum for  $e^\alpha \gg 1$ , as seen in in Figure 1 for for the case  $\alpha = 2$ . Conversely for  $e^\alpha \ll 1$  (negative  $\alpha$ ) the dip at  $\kappa^2 \simeq (5/2)A_2/A_1$ , which is already seen in the case of the initial Bunch-Davies vacuum state, becomes deeper since the imaginary term in Eq. (2.41) which remains non-zero is suppressed. The peak of the power spectrum in Figure 1 is enhanced for

$\alpha > 0$  since the amplitude of the scale-invariant spectrum as  $\kappa \rightarrow 0$  is suppressed relative to Bunch-Davies vacuum case ( $\alpha = 0$ )

$$\mathcal{P}_{\mathcal{R}} \rightarrow \frac{9e^{-2\alpha}H^6}{4\pi^2A_1^2}, \quad \text{for } \kappa \rightarrow 0, \quad (2.42)$$

$$\mathcal{P}_{\mathcal{R}} \rightarrow \frac{9e^{-2\alpha}H^6}{4\pi^2A_2^2}, \quad \text{for } \kappa \rightarrow \infty. \quad (2.43)$$

Finally, the late-time power spectrum (2.39) is shown for  $\alpha = 2$  and different values of  $\beta$  in Figure 2. For  $\beta \neq 0$  the rise of the power spectrum and the peak is less pronounced than for  $\beta = 0$ . For  $\beta \approx \pi$  there is again a dip in the power spectrum where the real part of  $\tilde{\mathcal{A}}_k - \tilde{\mathcal{B}}_k$  in Eq. (2.27) vanishes at  $\kappa^2 \simeq (5/2)A_2/A_1$  before the rise and the peak is suppressed, however we see that the dip moves to smaller values of  $\kappa$  for  $\alpha \sin \beta < 0$  (or larger values of  $\kappa$  for  $\alpha \sin \beta > 0$ ). In the rest of this paper we will focus on two specific values for the phase, corresponding to  $\beta = 0$  and  $\beta = \pi$ . Given the degeneracy between the sign of  $\alpha$  and the phase of  $\beta$  we will fix  $\beta = 0$  but consider both positive and negative values for  $\alpha$ .

### 2.1.3 Scalar-induced gravitational waves

While strong scale-dependent enhancements of the primordial scalar power spectrum have not been observed on the large, cosmological scales directly probed by the cosmic microwave background anisotropies, for example, they could be present on much smaller scales where they might be detectable through a scalar-induced stochastic gravitational wave background. At second-order in perturbation theory, the gravitational wave (GW) power spectrum depends quadratically on the first-order scalar power spectrum [45–48], so a scale-dependent feature in the scalar sector can also induce an enhancement and scale-dependence in the tensors. These second-order tensor perturbations could be much larger than those arising at first-order from the free fluctuations of the metric tensor [49, 50]. The dimensionless density of the induced GW background,  $\Omega_{GW}$ , is given by [49–52]:

$$\Omega_{GW,eq}(k) = 3 \int_0^\infty \int_{1+v}^{|1-v|} \frac{T(u,v)}{u^2v^2} \mathcal{P}_{\mathcal{R}}(vk) \mathcal{P}_{\mathcal{R}}(uk) du dv \quad (2.44)$$

where the kernel inside the integral is given by

$$T(u,v) = \frac{1}{4} \frac{1}{4v^2 - (1 + v^2 - u^2)^2} \frac{4uv}{u^2 + v^2 - 3} \times \left[ \ln \frac{3 - (u+v)^2}{3 - (u-v)^2} - \frac{4uv}{u^2 + v^2 - 3} + \pi^2 \Theta(u + v - \sqrt{3}) \right]. \quad (2.45)$$

We have used the publicly available code SIGWfast [34] to evaluate the GW density generated following a sudden transition in the Starobinsky piecewise linear model (2.16) for an initial  $\alpha$ -vacuum state (2.35). In the following numerical examples, we consider three different values for the parameter  $\alpha \in \{-2, 0, 2\}$  while fixing  $\beta = 0$ , as in the previous sub-section. As shown in Figure 3, we observe similar behaviour for  $\alpha = -2$  and  $\alpha = 0$ , with only minor variations in amplitude, consistent with previous findings for the BD vacuum case [40]. However, the positive- $\alpha$  scenario shows a strong enhancement over  $\alpha \leq 0$  at its peak and a subsequent decline  $\propto \kappa^{-3.5}$  with superimposed oscillations, before eventually converging to the same plateau as seen for  $\alpha \leq 0$ , but only at much smaller scales. This is a significant difference with respect to  $\alpha \leq 0$ , where the GW density shows only a small decrease for  $\kappa \gg 1$  from its peak near  $\kappa \sim 1$ .

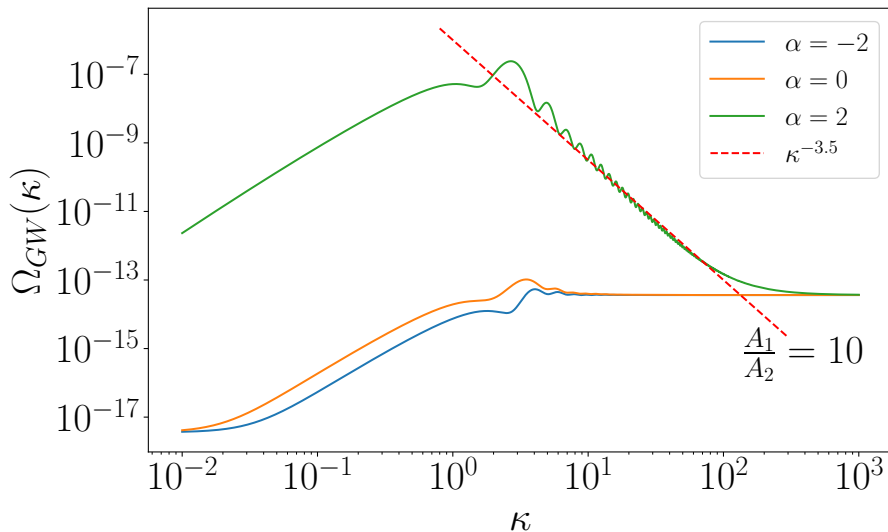


**Figure 3.** The gravitational waves energy density for the scalar induced gravitational waves  $\Omega_{GW}$  as a function of the normalized wavenumber  $\kappa = k/k_1$ , where  $k_1$  is the wavenumber which crosses the horizon at the sudden transition. The plot shows the different GW power spectra obtained from the scalar power spectra shown in Figure 1.

### 3 Generalization for multiple transitions

We have seen that the scalar power spectrum after a sudden transition can be significantly enhanced when considering an excited incoming state with  $\alpha > 0$  in Eq. (2.35). Thus it is interesting to explore the effect of multiple transitions during inflation, each of which will generate an excited state and can amplify any incoming excitations [4].

#### 3.1 $n$ transitions

In this section, we extend the Starobinsky model to encompass an arbitrary number of sudden transitions. As in the previous section 2.1, this generalized potential will be piece-wise linear:

$$V(\phi) = \begin{cases} V_1 + A_1(\phi - \phi_1), & \phi_1 < \phi \\ V_2 + A_2(\phi - \phi_2), & \phi_2 < \phi < \phi_1 \\ \dots \\ V_n + A_{n+1}(\phi - \phi_n), & \phi < \phi_n \end{cases}, \quad (3.1)$$

where  $V_{i+1} = V_i + A_{i+1}(\phi_{i+1} - \phi_i)$ , so that the potential is continuous at  $\phi = \phi_i$ , but with a discontinuous first derivative if  $A_{i+1} \neq A_i$ . We can adopt a methodology similar to that outlined in [40] to compute  $\dot{\phi}$  in each stage recursively. We will work again in the quasi-de Sitter limit where  $\epsilon_1 \rightarrow 0$  and we treat  $H$  as effectively constant. The Klein-Gordon equation (2.1) can then be rewritten for  $\phi_{i+1} < \phi < \phi_i$  as

$$\frac{d}{dt} \left( \dot{\phi} + \frac{A_{i+1}}{3H} \right) + 3H \left( \dot{\phi} + \frac{A_{i+1}}{3H} \right) = 0. \quad (3.2)$$

This has the simple solution

$$\dot{\phi} = -\frac{A_{i+1}}{3H} + \left( \dot{\phi}_i + \frac{A_{i+1}}{3H} \right) e^{-3H(t-t_i)} \quad (3.3)$$

where,  $t_i$  is the cosmic time at the  $i$ -th transition which occurs at  $\phi = \phi_i$  with velocity  $\dot{\phi} = \dot{\phi}_i$ . Although we previously assumed that field was in the slow-roll attractor,  $\dot{\phi} = -A_1/3H$ , before a single transition at  $\phi = \phi_1$ , this will not necessarily be the case at a second or subsequent transition at  $\phi = \phi_{i+1}$  for  $i \geq 1$  due to transient component, proportional to  $e^{-3Ht}$ , induced at the previous transition when  $\dot{\phi}_i \neq A_{i+1}/3H$ . Applying the simple solution (3.3) multiple times, we see that after  $i \geq 2$  transitions the field's velocity for  $\phi_{i+1} < \phi < \phi_i$  is given by

$$\dot{\phi} = -\frac{A_{i+1}}{3H} + \sum_{j=2}^i \frac{A_{j+1} - A_j}{3H} e^{-3H(t-t_j)} + \left( \dot{\phi}_1 + \frac{A_2}{3H} \right) e^{-3H(t-t_1)}. \quad (3.4)$$

If we assume that the field is in the slow-roll attractor for  $\phi > \phi_1$ , i.e., before the first transition, then this reduces to

$$\dot{\phi} = -\frac{A_{i+1}}{3H} + \sum_{j=1}^i \frac{A_{j+1} - A_j}{3H} e^{-3H(t-t_j)}. \quad (3.5)$$

We can now write down an expression for  $z(\tau) \equiv a\dot{\phi}/H$  after  $i \geq 2$  transitions:

$$z(\tau) = \frac{A_{i+1}}{3H^3\tau} - \left( \sum_{j=1}^i \frac{A_{j+1} - A_j}{3H^3\tau_j^3} \right) \tau^2. \quad (3.6)$$

Within each piece-wise linear phase,  $\phi_{i+1} < \phi < \phi_i$ , the time-dependent mass in the mode equation (2.5) remains invariant [37, 38],  $z''/z = 2/\tau^2$ , but it diverges at the transitions when  $\phi = \phi_i$  if  $A_{i+1} \neq A_i$ . The mode functions are thus given by the general solution (2.6) where  $f_k(\tau)$  in each phase is given by (2.19), but at each transition we must match the Bogoliubov coefficients, forming a chain of dependencies. The generalisation of the expression for the Bogoliubov coefficients after a single transition, Eq. (2.15), to each step in a series of multiple transitions for an arbitrary potential is

$$\begin{bmatrix} \mathcal{A}_{k,i+1} \\ \mathcal{B}_{k,i+1} \end{bmatrix} = \begin{bmatrix} 1 - i\Delta_i f_{k,i}^* f_{k,i}(2k)^{-1} & -i\Delta_i f_{k,i}^* f_{k,i}^*(2k)^{-1} \\ +i\Delta_i f_{k,i} f_{k,i}(2k)^{-1} & 1 + i\Delta_i f_{k,i}^* f_{k,i}(2k)^{-1} \end{bmatrix} \begin{bmatrix} \mathcal{A}_{k,i} \\ \mathcal{B}_{k,i} \end{bmatrix}, \quad (3.7)$$

where the generalisation of (2.9) at  $\phi = \phi_i$  gives

$$[z]_{i-}^{i+} = 0, \quad \left[ \frac{z'}{z} \right]_{i-}^{i+} = -\frac{a_i \Delta V'_i}{\dot{\phi}_i} \equiv \Delta_i. \quad (3.8)$$

Specialising again to the case of the piecewise linear potential (3.1), for a single transition where the field is initially in the slow-roll attractor approaching the transition at  $\phi = \phi_1$  then we have  $\dot{\phi}_1 = -A_1/3H$  and for  $i = 1$  we recover (2.23). More generally, where  $z(\tau)$  after  $i \geq 1$  transitions is given by Eq. (3.6), we have

$$\Delta_i = 3k_i (A_i - A_{i+1}) \left\{ A_i + \sum_{j=1}^{i-1} (A_j - A_{j+1}) \left( \frac{k_j}{k_i} \right)^3 \right\}^{-1}. \quad (3.9)$$

### 3.2 Two transitions

In this section, we apply the previous formulae for multiple transitions to the specific case of  $n = 2$  transitions in the Starobinsky piecewise-linear model (3.1). In this case, there are two values of the inflation field,  $\phi_1$  and  $\phi_2$ , at which the slope of the potential,  $V(\phi)$ , changes abruptly. The dynamics therefore can be split into three regimes. We assume that  $A_1 > 0$  and the field starts in the slow roll attractor (2.17) for  $\phi > \phi_1$ , while for  $\phi_2 < \phi < \phi_1$  or  $\phi < \phi_2$  the field velocity is given by Eq. (3.5). The general solution for the mode function is given by Eqs. (2.6) and (2.19), with arbitrary constants of integration,  $\mathcal{A}_{k,i}$  and  $\mathcal{B}_{k,i}$ , to be determined. We start with a de Sitter  $\alpha$ -vacuum state (corresponding to  $\beta = 0$  in (2.35)) and at each transition, we apply the Bogoliubov matching (3.7). In our numerical examples, we explore the effect on the power spectra of the choice of  $\alpha$  parameter for the initial quantum state and the two ratios between the different slopes in the three regimes. We fix the interval between the two transitions such that first  $k_2 = 30k_1$ , so the transitions are relatively well separated, but later we fix  $k_2 = 5k_1$  (such that the scalar field reaches the second transition at  $\phi_2$  when  $A_2 < 0$ ). We explore the primordial power spectrum (2.21) and resulting stochastic gravitational wave spectrum (2.44) in the different regimes:

- a) In Figures 4, 5, 6 we vary  $\alpha$  for different ratios between the potential gradients while keeping the slopes positive throughout ( $A_i > 0$ ). In each case, we see two distinct peaks, with steeper growth and much stronger enhancement, for  $\alpha > 0$ , as we saw for a single transition, whereas for  $\alpha \leq 0$  the first peak height is lower and the peak is much less clearly defined. The scalar power spectra in Figure 4, where  $A_2/A_3 = A_1/A_2$ , and Figure 6, where  $A_2/A_3 \gg A_1/A_2$ , are similar, both showing two main peaks for  $\alpha > 0$ , with the second peak at  $k/k_2 \simeq \pi$  (which corresponds to  $\kappa \simeq 30\pi$ ) higher than the first peak at  $\kappa = k/k_1 \simeq \pi$ . Meanwhile in Figure 5, where  $A_2/A_3 \ll A_1/A_2$ , the first peak is approximately the same height as the second peak for any  $\alpha$ . As a result  $\Omega_{GW}$  steadily increases to a single peak at  $\kappa \simeq 30\pi$  in Figures 4 and 6, while in Figure 5 the GW power spectrum has two approximately equal-height peaks for  $\alpha > 0$ , or an extended plateau for  $\alpha \leq 0$ .
- b) In Figures 7, 8 and 9, we explore the behaviour of the power spectra in cases where the inflationary potential is completely flat ( $A_2 = 0$ ) in the intermediate region  $\phi_2 < \phi < \phi_1$ , while allowing for different ratios for the initial and final slopes ( $A_1/A_3$ ). Note that in this case for the field to evolve beyond  $\phi_2$  we require  $\phi_1 - \phi_2 < A_1/9H^2$ , otherwise the field comes to a stop before reaching  $\phi_2$ . In all of the configurations that we investigate in Figures 7, 8 and 9 we find very similar results for the scalar power spectrum and for the GW power spectrum. As might be expected, the first peak height is more strongly enhanced in all cases compared with the equivalent case where  $A_2 > 0$ . As before, the two peaks, corresponding to the two transitions, are much more clearly defined when  $\alpha > 0$  and  $\Omega_{GW}$  is characterized by a double peak, where the second peak is slightly lower than the first one.
- c) Lastly, we explore in Figure 10 a configuration where the slope in the intermediate regime,  $A_2$ , takes a negative value. As for  $A_2 = 0$ , we must ensure that  $\phi_1 - \phi_2$  is small enough (or the transient velocity for  $\phi < \phi_1$  is large enough) that the field does indeed reach  $\phi_2$ . Otherwise, the field stops ( $\dot{\phi} = 0$ ) and it starts evolving back towards  $\phi_1$ , where it becomes trapped. This implies that for a given value of  $A_2 < 0$  the ratio  $k_2/k_1$

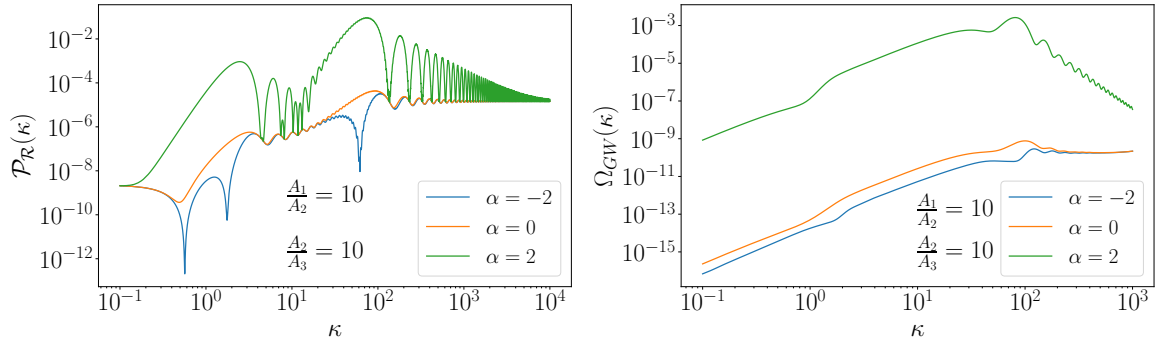


**Figure 4.** *Left:* The primordial power spectrum,  $\mathcal{P}_{\mathcal{R}}$ . *Right:* The dimensionless energy density for the scalar induced gravitational waves,  $\Omega_{GW}$ . Both spectra are shown as a function of the normalized wavenumber  $\kappa = k/k_1$  and the interval between the two transitions is given by the ratio  $k_2/k_1 = 30$ . We fix the ratios between the potential slopes  $A_1/A_2 = A_2/A_3 = 10$ , and set  $H^3 e^\alpha/A_1$  such that  $\mathcal{P}_{\mathcal{R}} \rightarrow 2 \times 10^{-9}$  for  $\kappa \rightarrow 0$ . The plots show different power spectra obtained by varying the value of the  $\alpha$  parameter in the initial  $\alpha$ -vacuum state.

is bounded from above; we require:

$$1 < \frac{k_2}{k_1} < \left(1 - \frac{A_1}{A_2}\right)^{1/3}. \quad (3.10)$$

For all values of  $\alpha$  we see a significant enhancement of the scalar power spectrum at the scale corresponding to the first transition ( $\kappa = 1$ ). When  $\alpha > 0$  there is a much steeper, greater enhancement and the power spectrum clearly drops before the second peak. This occurs even though we have set  $A_3 = A_1$  in this example, so that there is no overall change in slope between early and late times, with only a transient flat regime. Nonetheless, for any value of  $\alpha$  there is a strong effect on both the scalar and induced GW power spectra across a wide range of scales, e.g.,  $10^{-1} < \kappa < 10^4$  for  $\alpha = 2$ .

In all of the three cases discussed above, we can see that we obtain a distinctive structure of peaks in the power spectra corresponding to the frequencies at which the two transitions occur, with a positive value for  $\alpha$  distinguished by steeper growth, stronger enhancement, and two distinct peaks. In all cases, the scalar and tensor power spectra approach the same values in the low and high  $\kappa$  limits regardless of the value of  $\alpha$ . That is because we fix the normalisation at long wavelengths before the transition, while the asymptotic values at short wavelengths are then determined solely by the ratio of the initial and final slopes,  $A_3/A_1$ .

## 4 Conclusions

Models featuring sudden transitions in the scalar potential for curvature perturbations have attracted significant attention in recent years due to their key role in the possible production of primordial black holes and an associated scalar-induced gravitational wave background. Two key factors in determining the abundance and mass spectrum of PBHs as well as the spectrum of induced GWs are the height of the peaks in the power spectrum and the steepness of its growth. In this work, we have extended previous studies by considering a scenario where the quantum field originates in an excited state, specifically a de Sitter-invariant  $\alpha$ -vacuum [32]. Furthermore, we have studied a generalization of Starobinsky's piecewise-linear



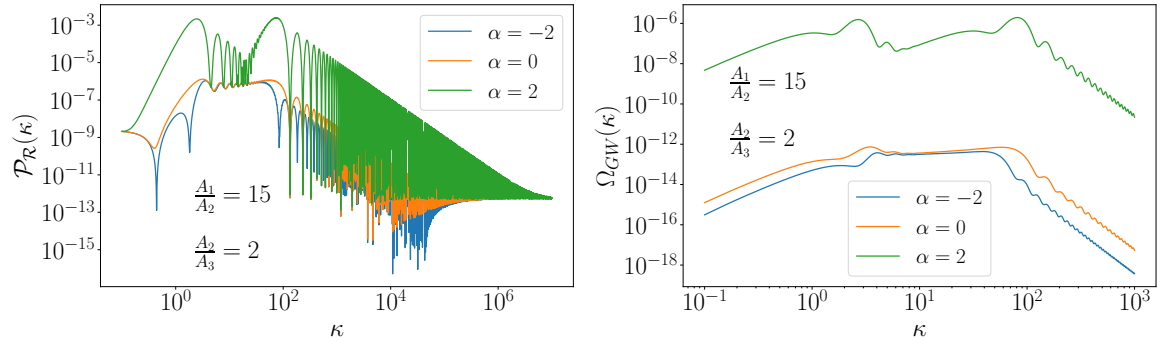


**Figure 5.** *Left:* The primordial power spectrum. *Right:* The gravitational waves energy density for the Scalar Induced Gravitational Waves  $\Omega_{GW}$ . Both the functions are shown as a function of the normalized wavenumber  $\kappa = k/k_1$  (where  $k_1$  is the wavenumber which crosses the horizon at the first transition) and the interval between the two transitions is given by the ratio  $k_2/k_1 = 30$ . In this case, we are setting the ratios between the regimes  $\frac{A_1}{A_2} = 15$  and  $\frac{A_2}{A_3} = 2$ . The plot shows different behaviour by varying the value of the  $\alpha$  parameter.

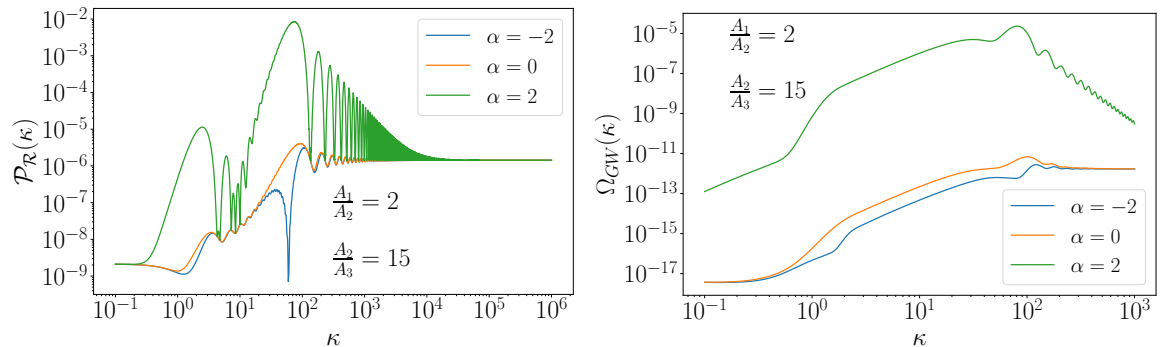


**Figure 6.** *Left:* The primordial power spectrum. *Right:* The gravitational waves energy density for the Scalar Induced Gravitational Waves  $\Omega_{GW}$ . Both the functions are plotted as a function of the normalized wavenumber  $\kappa = k/k_{T_1}$  at which the first transition happens. In this case, we are setting the ratios between the regimes  $\frac{A_1}{A_2} = 2$  and  $\frac{A_2}{A_3} = 15$ . The ratio of the wavenumbers corresponding to the two transitions is set to  $k_2/k_1 = 30$ . The plot shows different behaviour by varying the value of the  $\alpha$  parameter.

potential to include an arbitrary number of sudden transitions, providing an exact, order-by-order prescription for computing the Bogoliubov coefficients. These coefficients are sufficient to determine the primordial scalar power spectrum at the end of inflation. Our analytical results for a single sudden transition demonstrate a steep growth of the scalar power spectrum proportional to  $k^6$  for  $\alpha$ -vacua with  $\alpha > 0$ , in contrast to the expected growth proportional to  $k^4$  for an initial Bunch-Davies vacuum state where the  $\alpha$  parameter is set to zero. Since the scalar perturbations source primordial gravitational waves at second order, we have numerically calculated the resulting gravitational wave energy density. Our findings are consistent with the previous results in the literature for an initial Bunch-Davies vacuum while revealing a steeply peaked GW power spectrum for positive values of  $\alpha$ . These results are particularly interesting in light of the recent PTA results [53, 54] and possible observations with LISA [55] and other future GW detectors. For the case of two sudden transitions, we explored different possible combinations of the three slopes characterizing the generalized piecewise-



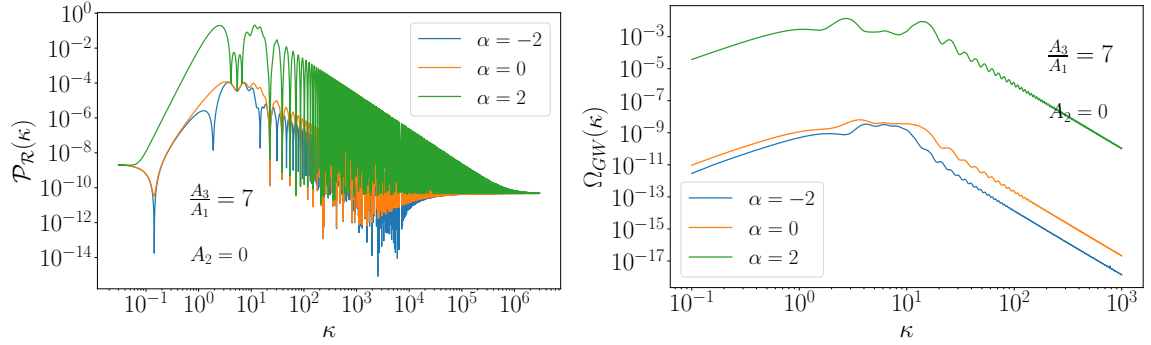


**Figure 7.** *Left:* The primordial power spectrum. *Right:* The gravitational waves energy density for the Scalar Induced Gravitational Waves  $\Omega_{GW}$ . Both the functions are plotted as a function of the normalized wavenumber  $\kappa = k/k_1$  at which the first transition happens. In this case, we are setting the ratios between the regimes  $\frac{A_3}{A_1} = 7$  while keeping  $A_2 = 0$ . The ratio of the wavenumbers corresponding to the two transitions is set to  $k_2/k_1 = 5$ . The plot shows different behaviour by varying the value of the  $\alpha$  parameter.

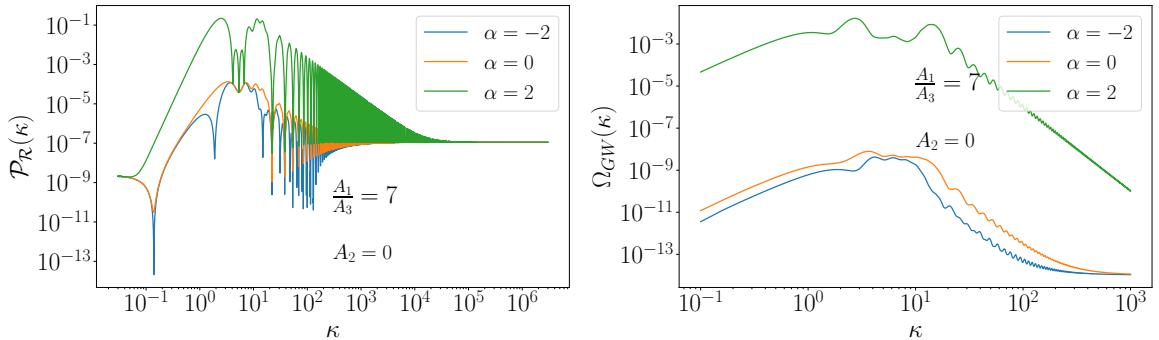


**Figure 8.** *Left:* The primordial power spectrum. *Right:* The gravitational waves energy density for the Scalar Induced Gravitational Waves  $\Omega_{GW}$ . Both the functions are plotted as a function of the normalized wavenumber  $\kappa = k/k_{T_1}$  at which the first transition happens. In this case, we are setting the ratios between the regimes  $A_3/A_1 = 1/7$  while keeping  $A_2 = 0$ . The ratio of the wavenumbers corresponding to the two transitions is set to  $k_2/k_1 = 5$ . The plot shows different behaviour by varying the value of the  $\alpha$  parameter.

linear potential. From the perspective of the curvature power spectrum, we demonstrated the possibility of generating multiple peaks with varying heights. For initial  $\alpha$ -vacua with  $\alpha > 0$  we find clearly separated peaks, whereas for  $\alpha \leq 0$  the initial peaks are less pronounced. Multiple peaks in the scalar power spectrum could lead to a non-trivial mass spectrum for PBHs which itself could lead to an interesting phenomenology. In all cases we have calculated the corresponding scalar-induced gravitational wave background, resulting in distinctive signal templates that could be tested by future experiments. These experiments may provide valuable insights into the initial quantum state of the universe. Our results suggest that localised features in the primordial scalar perturbations produced during sudden transitions during inflation could reveal information about both the nature of the transition and the incoming quantum state. Of course, it is unclear at this stage whether information about the initial state could be extracted from observations of gravitational relics such as PBHs and GWs independently of knowledge about the transition. We have only investigated instantaneous

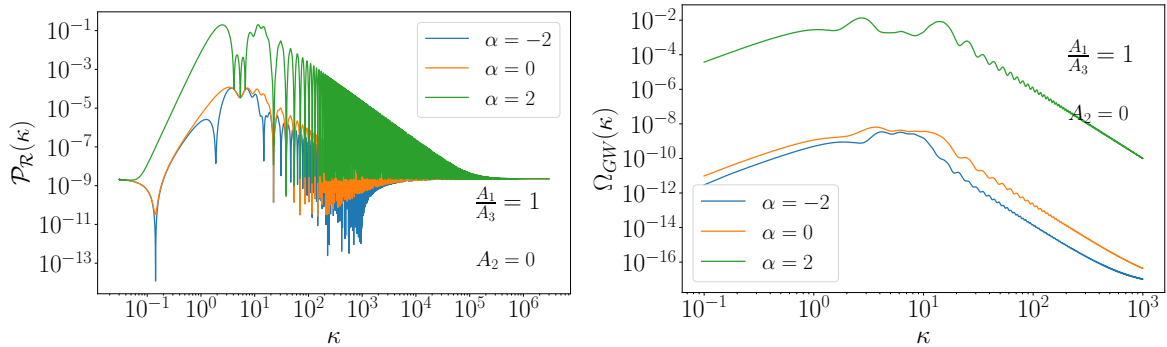


**Figure 9.** *Left:* The primordial power spectrum. *Right:* The gravitational waves energy density for the Scalar Induced Gravitational Waves  $\Omega_{GW}$ . Both the functions are plotted as a function of the normalized wavenumber  $\kappa = k/k_{T_1}$  at which the first transition happens. In this case, we are setting the ratios between the regimes  $\frac{A_1}{A_3} = 1$  while keeping  $A_2 = 0$ . The ratio of the wavenumbers corresponding to the two transitions is set to  $k_2/k_1 = 5$ . The plot shows different behaviour by varying the value of the  $\alpha$  parameter.

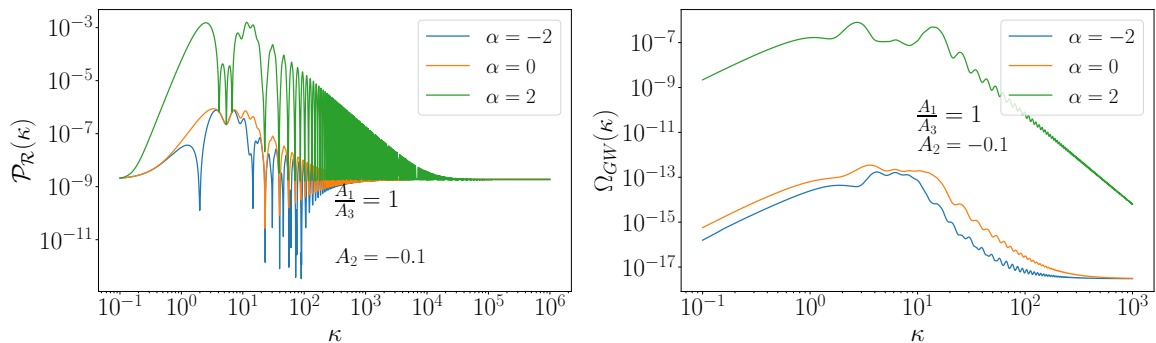


**Figure 10.** *Left:* The primordial power spectrum. *Right:* The gravitational waves energy density for the Scalar Induced Gravitational Waves  $\Omega_{GW}$ . Both the functions are plotted as a function of the normalized wavenumber  $\kappa = k/k_{T_1}$  at which the first transition happens. In this case, we are setting the ratios between the regimes  $\frac{A_1}{A_3} = 1$  while considering a negative value for  $A_2 = -0.1$ , consistent with the constraint. The ratio of the wavenumbers corresponding to the two transitions is set to  $k_2/k_1 = 5$ . The plot shows different behaviour by varying the value of the  $\alpha$  parameter.

models of the transition in this paper, and we know this will give spurious effects on arbitrarily small scales. Any finite duration of the transition,  $\Delta t$ , is expected to smooth out structures on a scale  $k \gg a/\Delta t$ . The resulting abundance of PBHs can also be very sensitive to non-Gaussianity in the density distribution [56–63], which arise from higher-order corrections to the linear analysis of perturbations used in this paper. Indeed non-perturbative techniques are ultimately needed to study very large, very rare perturbations which lead to PBHs [64–68]. It would be interesting to extend our study of non-Bunch-Davies initial quantum states to such non-linear analyses.

## Acknowledgments

M. C. is grateful to the Insitute of Cosmology and Gravitation for hospitality and support. The work of M. C. is supported by the “Angelo Della Riccia” Fellowship. The work of M. C.,

G. M., and O. P. is partially supported by the INFN “Theoretical Astroparticle Physics” (TAsP) project. O. P. and G. M. acknowledge support by Ministero dell’Universit’a e della Ricerca (MUR), PRIN2022 program (Grant PANTHEON 2022E2J4RK) Italy. D.W. was supported by the Science and Technology Facilities Council (grant number ST/W001225/1). For the purpose of open access, the authors have applied a Creative Commons Attribution (CC-BY) licence to any Author Accepted Manuscript version arising from this work.

## References

- [1] C.T. Byrnes, P.S. Cole and S.P. Patil, *Steepest growth of the power spectrum and primordial black holes*, *JCAP* **06** (2019) 028 [[1811.11158](#)].
- [2] P. Carrilho, K.A. Malik and D.J. Mulryne, *Dissecting the growth of the power spectrum for primordial black holes*, *Phys. Rev. D* **100** (2019) 103529 [[1907.05237](#)].
- [3] O. Özsoy and G. Tasinato, *Inflation and Primordial Black Holes*, *Universe* **9** (2023) 203 [[2301.03600](#)].
- [4] G. Tasinato, *An analytic approach to non-slow-roll inflation*, *Phys. Rev. D* **103** (2021) 023535 [[2012.02518](#)].
- [5] G. Ballesteros, S. Céspedes and L. Santoni, *Large power spectrum and primordial black holes in the effective theory of inflation*, *JHEP* **01** (2022) 074 [[2109.00567](#)].
- [6] P.S. Cole, A.D. Gow, C.T. Byrnes and S.P. Patil, *Steepest growth re-examined: repercussions for primordial black hole formation*, [2204.07573](#).
- [7] R. Zhai, H. Yu and P. Wu, *Power spectrum with  $k^6$  growth for primordial black holes*, *Phys. Rev. D* **108** (2023) 043529 [[2308.09286](#)].
- [8] LISA COSMOLOGY WORKING GROUP collaboration, *Primordial black holes and their gravitational-wave signatures*, [2310.19857](#).
- [9] J. Garcia-Bellido, A.D. Linde and D. Wands, *Density perturbations and black hole formation in hybrid inflation*, *Phys. Rev. D* **54** (1996) 6040 [[astro-ph/9605094](#)].
- [10] A.M. Green and B.J. Kavanagh, *Primordial Black Holes as a dark matter candidate*, *J. Phys. G* **48** (2021) 043001 [[2007.10722](#)].
- [11] A. Escrivà, F. Kuhnel and Y. Tada, *Primordial Black Holes*, [2211.05767](#).
- [12] P. Ivanov, P. Naselsky and I. Novikov, *Inflation and primordial black holes as dark matter*, *Phys. Rev. D* **50** (1994) 7173.
- [13] W.H. Kinney, *Horizon crossing and inflation with large eta*, *Phys. Rev. D* **72** (2005) 023515 [[gr-qc/0503017](#)].
- [14] J. Garcia-Bellido, M. Peloso and C. Unal, *Gravitational Wave signatures of inflationary models from Primordial Black Hole Dark Matter*, *JCAP* **09** (2017) 013 [[1707.02441](#)].
- [15] H. Motohashi and W. Hu, *Primordial Black Holes and Slow-Roll Violation*, *Phys. Rev. D* **96** (2017) 063503 [[1706.06784](#)].
- [16] P.S. Cole, A.D. Gow, C.T. Byrnes and S.P. Patil, *Primordial black holes from single-field inflation: a fine-tuning audit*, *JCAP* **08** (2023) 031 [[2304.01997](#)].
- [17] J.H.P. Jackson, H. Assadullahi, A.D. Gow, K. Koyama, V. Vennin and D. Wands, *The separate-universe approach and sudden transitions during inflation*, [2311.03281](#).
- [18] M. Cielo, G. Mangano and O. Pisanti, *Impact of trans-Planckian quantum noise on the primordial gravitational wave spectrum*, *Phys. Rev. D* **108** (2023) 043501 [[2211.04316](#)].

- [19] M. Cielo, M. Fasiello, G. Mangano and O. Pisanti, *Gravitational Wave non-Gaussianity from trans-Planckian Quantum Noise*, [2309.12285](#).
- [20] R. Holman and A.J. Tolley, *Enhanced Non-Gaussianity from Excited Initial States*, *JCAP* **05** (2008) 001 [[0710.1302](#)].
- [21] Y. Yin, *The cosmological collider signal in the non-BD initial states*, [2309.05244](#).
- [22] A. Ashoorioon, K. Dimopoulos, M.M. Sheikh-Jabbari and G. Shiu, *Non-Bunch–Davis initial state reconciles chaotic models with BICEP and Planck*, *Phys. Lett. B* **737** (2014) 98 [[1403.6099](#)].
- [23] S. Kanno and M. Sasaki, *Graviton non-gaussianity in  $\alpha$ -vacuum*, *JHEP* **08** (2022) 210 [[2206.03667](#)].
- [24] G.L. Alberghi, R. Casadio and A. Tronconi, *TransPlanckian footprints in inflationary cosmology*, *Phys. Lett. B* **579** (2004) 1 [[gr-qc/0303035](#)].
- [25] S. Kundu, *Inflation with General Initial Conditions for Scalar Perturbations*, *JCAP* **02** (2012) 005 [[1110.4688](#)].
- [26] R.H. Brandenberger and J. Martin, *Trans-Planckian Issues for Inflationary Cosmology*, *Class. Quant. Grav.* **30** (2013) 113001 [[1211.6753](#)].
- [27] T. Tanaka, *A Comment on transPlanckian physics in inflationary universe*, [astro-ph/0012431](#).
- [28] H. Bouzari Nezhad and F. Shojai, *The Effect of  $\alpha$ -Vacua on the Scalar and Tensor Spectral Indices: Slow-Roll Approximation*, *Phys. Rev. D* **98** (2018) 063512 [[1802.05537](#)].
- [29] S. Akama, S. Hirano and T. Kobayashi, *Primordial tensor non-Gaussianities from general single-field inflation with non-Bunch-Davies initial states*, *Phys. Rev. D* **102** (2020) 023513 [[2003.10686](#)].
- [30] A. Shukla, S.P. Trivedi and V. Vishal, *Symmetry constraints in inflation,  $\alpha$ -vacua, and the three point function*, *JHEP* **12** (2016) 102 [[1607.08636](#)].
- [31] J. Lesgourgues, D. Polarski and A.A. Starobinsky, *Quantum to classical transition of cosmological perturbations for nonvacuum initial states*, *Nucl. Phys. B* **497** (1997) 479 [[gr-qc/9611019](#)].
- [32] B. Allen, *Vacuum States in de Sitter Space*, *Phys. Rev. D* **32** (1985) 3136.
- [33] A.A. Starobinsky, *Spectrum of adiabatic perturbations in the universe when there are singularities in the inflation potential*, *JETP Lett.* **55** (1992) 489.
- [34] L.T. Witkowski, *SIGWfast: a python package for the computation of scalar-induced gravitational wave spectra*, [2209.05296](#).
- [35] K. Dimopoulos, *Ultra slow-roll inflation demystified*, *Phys. Lett. B* **775** (2017) 262 [[1707.05644](#)].
- [36] V. Mukhanov and S. Winitzki, *Introduction to quantum effects in gravity*, Cambridge University Press (6, 2007).
- [37] D. Wands, *Duality invariance of cosmological perturbation spectra*, *Phys. Rev. D* **60** (1999) 023507 [[gr-qc/9809062](#)].
- [38] S.M. Leach, M. Sasaki, D. Wands and A.R. Liddle, *Enhancement of superhorizon scale inflationary curvature perturbations*, *Phys. Rev. D* **64** (2001) 023512 [[astro-ph/0101406](#)].
- [39] M. Maggiore, *Gravitational Waves. Vol. 2: Astrophysics and Cosmology*, Oxford University Press (3, 2018).
- [40] S. Pi and J. Wang, *Primordial black hole formation in Starobinsky’s linear potential model*, *JCAP* **06** (2023) 018 [[2209.14183](#)].

- [41] U.H. Danielsson, *A Note on inflation and transPlanckian physics*, *Phys. Rev. D* **66** (2002) 023511 [[hep-th/0203198](#)].
- [42] B.J. Broy, *Corrections to  $n_s$  and  $n_t$  from high scale physics*, *Phys. Rev. D* **94** (2016) 103508 [[1609.03570](#)].
- [43] D.H. Lyth and A. Riotto, *Particle physics models of inflation and the cosmological density perturbation*, *Phys. Rept.* **314** (1999) 1 [[hep-ph/9807278](#)].
- [44] D.J.H. Chung, E.W. Kolb, A. Riotto and I.I. Tkachev, *Probing Planckian physics: Resonant production of particles during inflation and features in the primordial power spectrum*, *Phys. Rev. D* **62** (2000) 043508 [[hep-ph/9910437](#)].
- [45] K. Tomita, *Non-Linear Theory of Gravitational Instability in the Expanding Universe*, *Prog. Theor. Phys.* **37** (1967) 831.
- [46] S. Matarrese, O. Pantano and D. Saez, *A General relativistic approach to the nonlinear evolution of collisionless matter*, *Phys. Rev. D* **47** (1993) 1311.
- [47] S. Matarrese, O. Pantano and D. Saez, *General relativistic dynamics of irrotational dust: Cosmological implications*, *Phys. Rev. Lett.* **72** (1994) 320 [[astro-ph/9310036](#)].
- [48] S. Matarrese, S. Mollerach and M. Bruni, *Second order perturbations of the Einstein-de Sitter universe*, *Phys. Rev. D* **58** (1998) 043504 [[astro-ph/9707278](#)].
- [49] K.N. Ananda, C. Clarkson and D. Wands, *The Cosmological gravitational wave background from primordial density perturbations*, *Phys. Rev. D* **75** (2007) 123518 [[gr-qc/0612013](#)].
- [50] D. Baumann, P.J. Steinhardt, K. Takahashi and K. Ichiki, *Gravitational Wave Spectrum Induced by Primordial Scalar Perturbations*, *Phys. Rev. D* **76** (2007) 084019 [[hep-th/0703290](#)].
- [51] G. Domènech, *Scalar Induced Gravitational Waves Review*, *Universe* **7** (2021) 398 [[2109.01398](#)].
- [52] J. Fumagalli, G.A. Palma, S. Renaux-Petel, S. Sypsas, L.T. Witkowski and C. Zenteno, *Primordial gravitational waves from excited states*, *JHEP* **03** (2022) 196 [[2111.14664](#)].
- [53] NANOGrav collaboration, *The NANOGrav 15 yr Data Set: Evidence for a Gravitational-wave Background*, *Astrophys. J. Lett.* **951** (2023) L8 [[2306.16213](#)].
- [54] NANOGrav collaboration, *The NANOGrav 15 yr Data Set: Search for Signals from New Physics*, *Astrophys. J. Lett.* **951** (2023) L11 [[2306.16219](#)].
- [55] LISA COSMOLOGY WORKING GROUP collaboration, *Cosmology with the Laser Interferometer Space Antenna*, *Living Rev. Rel.* **26** (2023) 5 [[2204.05434](#)].
- [56] J.S. Bullock and J.R. Primack, *NonGaussian fluctuations and primordial black holes from inflation*, *Phys. Rev. D* **55** (1997) 7423 [[astro-ph/9611106](#)].
- [57] S. Young and C.T. Byrnes, *Primordial black holes in non-Gaussian regimes*, *JCAP* **08** (2013) 052 [[1307.4995](#)].
- [58] C.-M. Yoo, J.-O. Gong and S. Yokoyama, *Abundance of primordial black holes with local non-Gaussianity in peak theory*, *JCAP* **09** (2019) 033 [[1906.06790](#)].
- [59] M. Biagetti, V. De Luca, G. Franciolini, A. Kehagias and A. Riotto, *The formation probability of primordial black holes*, *Phys. Lett. B* **820** (2021) 136602 [[2105.07810](#)].
- [60] N. Kitajima, Y. Tada, S. Yokoyama and C.-M. Yoo, *Primordial black holes in peak theory with a non-Gaussian tail*, *JCAP* **10** (2021) 053 [[2109.00791](#)].
- [61] G. Ferrante, G. Franciolini, A. Iovino, Junior. and A. Urbano, *Primordial non-Gaussianity up to all orders: Theoretical aspects and implications for primordial black hole models*, *Phys. Rev. D* **107** (2023) 043520 [[2211.01728](#)].

- [62] A.D. Gow, H. Assadullahi, J.H.P. Jackson, K. Koyama, V. Vennin and D. Wands, *Non-perturbative non-Gaussianity and primordial black holes*, *EPL* **142** (2023) 49001 [[2211.08348](#)].
- [63] T. Matsubara and M. Sasaki, *Non-Gaussianity effects on the primordial black hole abundance for sharply-peaked primordial spectrum*, *JCAP* **10** (2022) 094 [[2208.02941](#)].
- [64] C. Pattison, V. Vennin, H. Assadullahi and D. Wands, *Quantum diffusion during inflation and primordial black holes*, *JCAP* **10** (2017) 046 [[1707.00537](#)].
- [65] M. Biagetti, G. Franciolini, A. Kehagias and A. Riotto, *Primordial Black Holes from Inflation and Quantum Diffusion*, *JCAP* **07** (2018) 032 [[1804.07124](#)].
- [66] J.M. Ezquiaga, J. García-Bellido and V. Vennin, *The exponential tail of inflationary fluctuations: consequences for primordial black holes*, *JCAP* **03** (2020) 029 [[1912.05399](#)].
- [67] S. Pi and M. Sasaki, *Logarithmic Duality of the Curvature Perturbation*, *Phys. Rev. Lett.* **131** (2023) 011002 [[2211.13932](#)].
- [68] Y.-F. Cai, X.-H. Ma, M. Sasaki, D.-G. Wang and Z. Zhou, *Highly non-Gaussian tails and primordial black holes from single-field inflation*, *JCAP* **12** (2022) 034 [[2207.11910](#)].